

Short communication

Simple synthesis of Pt nanoparticles on noncovalent functional MWNT surfaces: Application in ethanol electrocatalysis

Guoyu Gao, Guangwu Yang, Maowen Xu, Ce Wang, Cailing Xu*, Hulin Li*

College of Chemistry and Chemical Engineering, Lanzhou University, Lanzhou 730000, PR China

Received 27 January 2007; received in revised form 14 June 2007; accepted 24 June 2007

Available online 29 June 2007

Abstract

After the siloxane is polymerized on the nanotube surfaces, the carbon nanotube is embedded within the polysiloxane shell with a hydrophilic amino group situated outside. Platinum (Pt) nanoparticles were synthesised on as-produced noncovalent functional multi-walled carbon nanotubes (MWNTs) via electrostatic interactions. The structure and nature of the resulting Pt/MWNT composite were characterized by transmission electron microscopy (TEM) and X-ray diffraction (XRD). The electrocatalytic properties of the Pt/MWNT electrode for oxidation of ethanol have been investigated by cyclic voltammetry (CV), and excellent electrocatalytic activity can be observed.

© 2007 Published by Elsevier B.V.

Keywords: Si-MWNTS; Platinum particles; Ethanol oxidation

1. Introduction

Carbon nanotubes (CNTs), as a new form of carbon, have attracted considerable attention due to their unique structure, electrical and mechanical properties [1–7]. The physical and chemical properties of CNTs offer unprecedented opportunities of novel applications that are dependent on the electronic conductivity in terms of nanotube diameters and surface properties. Indeed, in the past several years, a variety of potential applications of CNTs have been explored, including catalysis, sensors, and biosensors [8–12]. A number of strategies have also been developed for the surface modification of CNTs by functional groups and functional-group-anchored nanoparticles [13,14].

Recently, many attempts have been conducted to deposit various metal particles onto the surface of CNTs for their application in the area of catalysis. Some metals and their compounds, such as Pt, Pd, Ag, Au, Ni, Fe, have been deposited on the CNTs successfully [15–20]. Among these metals, Pt and Pt group metals are considered to be the most frequently employed catalyst materials for the electrochemical reactions in full cells. He et al. took advantage of the high purity of electrochemi-

cally deposited nanoparticles to decorate CNTs with bimetallic Pt–Ru nanoparticles with diameters of 60–80 nm [21]. Yu et al. obtained a well-dispersed deposition of Pt clusters on the surface of CNTs via acid groups as specific nucleation sites [22]. All of these methods were very useful and except for some limitations, for example difficult large-scale synthesis of modified CNT or causing damages to the tubular structure. Therefore, to develop a method to synthesize Pt/MWNTs in easy and timesaving is still a challenge. Lin et al. demonstrate a novel synthetic route towards selective heterogeneous metal nucleation and growth on modified and unmodified CNTs [23].

In this paper, a novel method has been described for preparation of Pt nanoparticles through noncovalent functionalization of MWNTs, analogous to the procedure employed to disperse Au particles on MWNTs in the literature [24] as shown in Fig. 1. First, embedding the nanotubes within siloxane by hydrophobic interaction; then the siloxane micelles were cross-linked with Si–O–Si framework by addition of hydrochloric acid [25]; such a structure probably originates from the formation of the micelle in which ammonium groups extrude outside. Therefore, the formation of an ion complex is required because the ion complex has strong hydrophilicity. Finally, a PtCl_6^{2-} monolayer was adsorbed onto the modified MWNT surface by electrostatic interaction and Pt nanoparticles were obtained by reduction. This strategy has several advantages. (1) Modified MWNT surface

* Corresponding author. Tel.: +86 931 891 2517; fax: +86 931 891 2582.
E-mail address: lihl@lzu.edu.cn (H. Li).

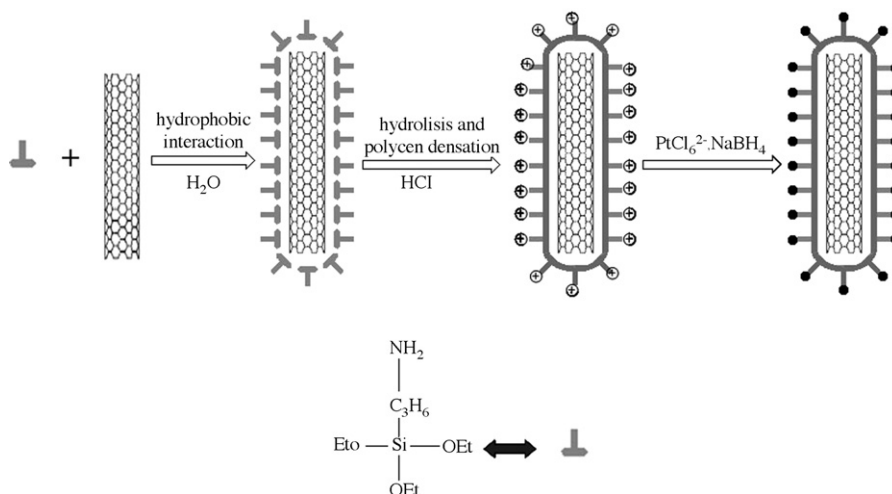


Fig. 1. Schematic procedure for the preparation of Pt nanoparticles on noncovalent functional MWNTs.

via hydrophobic interaction which is easy and rapid process. (2) The amine groups on MWNT surfaces provide a uniform functional surface, which can effectively prevent the preferred nucleation process on the MWNT surface. (3) The specific electrostatic interaction between the substrate and adsorbed atom can cause particle size distributions to be considerably narrower than in the case of random nucleation. (4) This method is generally very simple to implement and is thus an attractive choice for large-scale synthesis.

The electrocatalytic activity of Pt/Si-MWNTs for ethanol oxidation was also investigated in detail.

2. Experimental

2.1. Noncovalent functionalization of MWNTs with polysiloxane

MWNTs were purchased from Nanotech Port Ltd. Co. (Shenzhen, China). The samples were purified by procedures already reported in the literature [26,27]. Thirty milligrams of MWNTs were added to 60.00 mL of distilled water and could not be well dispersed by ultrasonication in a laboratory ultrasonic bath. Then, with the addition of 3 mL 3-APTES and ultrasonicate for 10 min, a homogeneous, well-dispersed suspension could be easily prepared. Next, the siloxane micelles were cross-linked with Si–O–Si framework by addition of 2 mL of hydrochloric acid (0.1 M). After the cross-linking of siloxane, excess reagents were removed by dialysis of the suspension against distilled water. The polysiloxane-embedded MWNTs (Si-MWNTs) were purified from the suspension by several cycles of centrifuging the suspension and discarding the supernatant. The Si-MWNTs were dried in a vacuum oven at 50 °C for about 2 h for further use. The dispersibility of carbon nanotubes in water can be attributed to the presence of a large numbers of amino groups on the surfaces of the carbon nanotubes.

2.2. Preparation of Pt/Si-MWNTs catalyst electrode

Ten milligrams of purified Si-MWNTs was dispersed in 30.00 mL of distilled water and mixed with 0.4 mL of

$\text{H}_2\text{PtCl}_6 \cdot 6\text{H}_2\text{O}$ (77.8 mM) aqueous solution for 0.5 h. During this period, the negatively charged PtCl_6^{2-} was anchored on the surface of Si-MWNTs through electrostatic interaction. Next, 0.5 mL of 0.07 M NaBH_4 aqueous solution was added in with stirring. After centrifugation, the black solids left at bottom of the container were extensively washed with distilled water to remove free Pt nanoparticles several times.

Five milligrams of Pt/Si-MWNTs catalyst, 50 μL of Nafion solution (5 wt%, Aldrich) and 1.0 mL of alcohol were mixed. A measured volume (ca. 25 μL) of this mixture was transferred via a syringe onto a glassy carbon electrode and heated under an infrared lamp to remove the solvent.

2.3. Measurements

UV–vis absorption spectra were recorded on a Hitachi U-3010 spectrometer.

The morphology of synthesized nanoparticles was observed on a Hitachi 600 transmission electron microscopy (TEM). The samples were prepared by dipping the Pt/Si-MWNTs aqueous solution on the Cu grids and observed at 100 kV.

X-ray diffraction (XRD) data from the samples were collected using a Rigaku D/MAX 24000 diffractometer with $\text{Cu K}\alpha$ radiation.

Electrochemical measurements were performed with BAS100B electrochemical analyzer (USA), a conventional cell with a three-electrode configuration was used throughout this work. The working electrode is a Pt/Si-MWNTs/GCE (glassy carbon electrode), platinum foil was used as counter electrode, and saturated calomel electrode (SCE) was reference electrode. All potentials were measured and reported with respect to SCE in this paper. All measurements were performed at room temperature.

3. Results and discussion

3.1. UV–vis analysis of the Pt/Si-MWNTs catalyst

The formation of Pt nanoparticles via noncovalent functional Si-MWNT was followed by UV–vis spectroscopy. In Fig. 2a, the

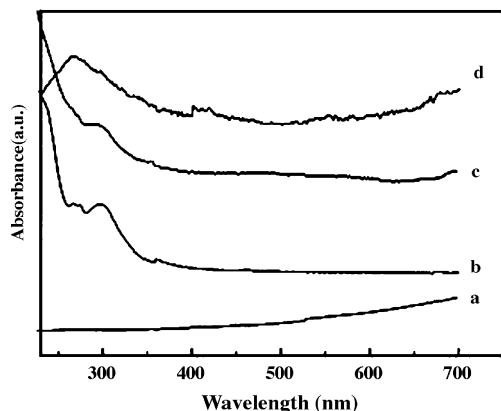


Fig. 2. UV-vis absorption spectra of MWNTs (a), 3-APTES (b), Si-MWNTs (c) and Pt nanoparticles attached to the Si-MWNT surfaces (d) in distilled water, respectively.

pristine MWNTs present a typical featureless spectrum, while the adsorption peak of 3-APTES appears at 300 nm (Fig. 2b). The absorption spectrum of Si-MWNT reveals additional features corresponding to 3-APTES at about 300 nm (Fig. 2c). The existence of these characteristic 3-APTES peak in Si-MWNTs strongly suggests the noncovalent modification of 3-APTES on the pristine MWNT surfaces. Fig. 2d is the spectra of Si-MWNT after being attached with Pt nanoparticles. The peak appears blue-shift as compared to the peak in Fig. 2c. This can be due to the particle interactions absorbed on the Si-MWNTs. Hence, we can concluded that the Pt nanoparticles are bound to the Si-MWNT surface.

3.2. TEM analysis of the Pt/Si-MWNTs catalyst

It is well known that the MWNTs produced by the chemical vapor deposition method are accompanied with many metal catalysts, support materials and amorphous carbon. Therefore, it is necessary to use some surface treatment onto the MWNTs. Fig. 3a shows the TEM image of the purified MWNTs treated with concentrated hydrochloride acid. All of the tubes are very clean. It can be seen that the MWNTs are very long and present as a highly entangled network structure. Compared to Fig. 3a, the purified Si-MWNTs in distilled water is not clear like the former (Fig. 3b), they seem to be decorated in the siloxane film, and many black dots appears at the side-walls of MWNTs. This attributed to the presence of polysiloxane on MWNT surface. Obviously, the siloxane contains individual MWNT rather than MWNTs bundles. The direct evidence of the Pt nanoparticles on the surface of Si-MWNT was given by Fig. 3c. It can be seen that well-dispersed, spherical particles were anchored onto the external walls of MWNTs and the size range of these particles was 3–10 nm. During the preparation of Pt nanoparticles, they were formed with bare surface in the large image of Fig. 3d. After have been anchored on the Si-MWNT surface, the Pt nanoparticles are acted as core to grow up, which lead to some aggregation between adjacent particles (Fig. 3e)

3.3. XRD analysis of Pt/SWNT composites

The X-ray power diffraction (XRD) spectrum of Pt/Si-MWNTs composites is shown in Fig. 4. The MWNTs showed

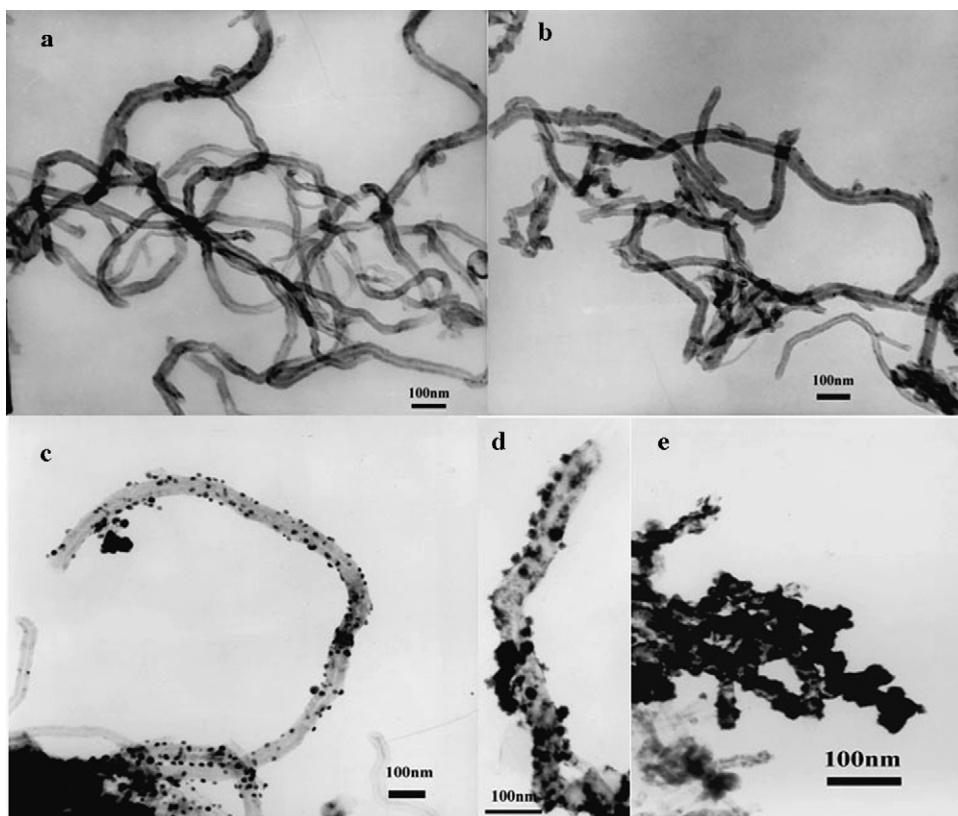


Fig. 3. TEM image of pristine MWNT (a), Si-MWNTs (b), Pt/Si-MWNTs (c and d) and Pt/Si-MWNTs with long time (e).

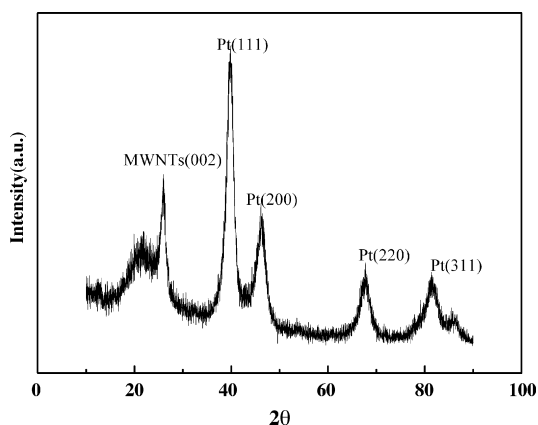


Fig. 4. Powder X-ray diffraction (XRD) pattern of Pt/Si-MWNTs composites.

typical peak of (002) phase of MWNTs or graphite. It clearly shows the five main characteristic peaks of the face-centered cubic (fcc) crystalline Pt and has major peaks of Pt(111) at 39.7° , Pt(200) at 46.3° , Pt(220) at 67.5° , Pt(311) at 81.2° , Pt(222) at 85.7° , indicating the successful reduction of metal salt to Pt. The average size of the Pt particles is 5.7 nm calculated by the Scherrer formula, which is in good agreement with the results by the TEM image.

3.4. Electrochemical properties of Pt/Si-MWNTs composites

Fig. 5 shows the typical cyclic voltammograms of Pt/Si-MWNTs and MWNT deposited on glassy carbon electrode in 1 M C_2H_5OH + 0.5 M H_2SO_4 aqueous solutions. For curve A, the background current is much larger due to the high surface area of MWNT. On the other hand, the oxidation and reduction peaks are observed obviously at 0.22 and 0.41 V. It may correlate with the redox behavior of carboxylic acid groups, which imply that the surface of MWNTs has been activated by electrochemical treatment in 0.5 M H_2SO_4 . But no current peaks of ethanol oxidation are observed from curve (A) in Fig. 5, which indicates that the MWNT grafted glassy carbon electrode have no electrocatalytic activity for ethanol oxidation. From curve (B) in

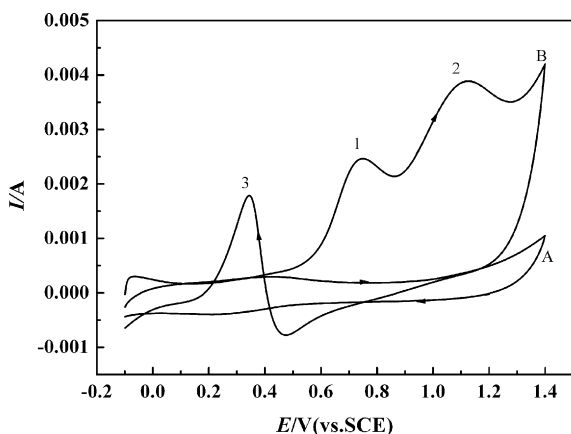


Fig. 5. Cyclic voltammograms of 1 M C_2H_5OH in 0.5 M H_2SO_4 at MWNT (A) and Pt/Si-MWNTs (B) composite electrodes.

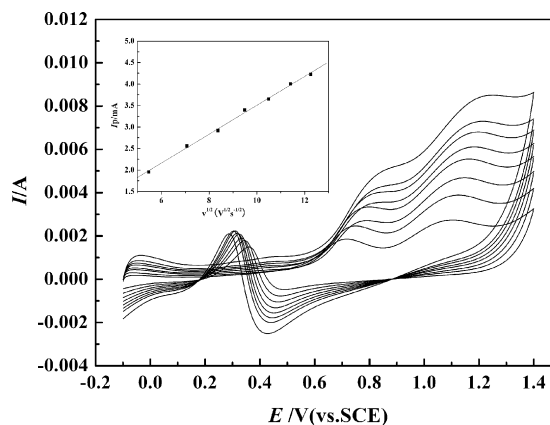


Fig. 6. Voltammograms of 1 M C_2H_5OH in 0.5 M H_2SO_4 solutions. Scan rate: 30, 50, 70, 90, 110, 130, 150 and 200 $mV s^{-1}$ from inner to outer.

Fig. 5, three peaks of ethanol oxidation can be observed and the peak potential are 0.64, 1.12 and 0.32 V, respectively. Two oxidation peaks were found during the forward sweep, according to the literature [28,29], the first peak (1) corresponding mainly to the formation of CO_2 , The first peak appears in a region of potentials when OH bonded to the Pt surface quickly, The formation of OH species plays an important role during the ethanol oxidation with break of the C–C bond, the producing CO_2 via the CO strongly adsorbed on the platinum substrate [30,31], whereas the second oxidation peak (2) corresponding mainly to the formation of CH_3CHO the product (c) is still unclear. Additionally, the ratio of $i_p(1)/i_p(2)$ is used to evaluate the conversion extent from ethanol to CO_2 . From Fig. 5B, the ratio value can be calculated and equal to 0.65 for Pt/Si-MWNTs composite electrode, which is higher than that of the other catalysts [32]. The potential of peak c is more negative than that of the other catalysts [33]. This maybe attributed to the high dispersion of platinum catalysts and effective functionalization of MWNTs.

Fig. 6 shows the Voltammograms of 1 M C_2H_5OH in 0.5 M H_2SO_4 solutions at various scan rates. The current of peak 3 was linearly proportional to the square root of scan rate within some range, which indicate the oxidation maybe controlled by a diffusion process in a range of scan rates. Additionally, the peaks 1 and 2 shift positively with the increasing scan rates while peak 3 shift negatively. This demonstrates that the oxidation of peak 3 become much easy.

4. Conclusions

A novel approach has been developed to synthesize Pt/Si-MWNTs composite by noncovalent Si-MWNT surface within polysiloxane. The UV–vis absorption spectrum of Pt/Si-MWNTs elucidates the noncovalent binding of 3-APTES on the pristine MWNT surfaces. TEM studies show that well-dispersed, spherical particles were anchored onto the external walls of Si-MWNTs, and the size range of these particles was about 3–10 nm. Additionally, Pt/Si-MWNT composites exhibit excellent catalytic activity for ethanol oxidation. This simple, rapid and green nanoparticle deposition technique is not limit to

Au, Pt; it could be used to prepare a variety of metal nanoparticles on MWNTs for application as catalysts in fuel cells.

References

- [1] S. Iijima, *Nature* 354 (1991) 56.
- [2] T.W. Ebbesen, H.J. Lezec, H. Hiura, J.W. Bennett, H.F. Ghaemi, T. Thio, *Nature* 382 (1996) 54.
- [3] H. Dai, J.H. Hafner, A.G. Rinzler, D.T. Colbert, R. Smalley, *Nature* 384 (1996) 147.
- [4] Z. Liu, X. Lin, J.Y. Lee, W. Zhang, M. Han, L.M. Gan, *Langmuir* 18 (2002) 4054.
- [5] M. Terrones, *Int. Mater. Rev.* 49 (2004) 325.
- [6] C.A. Dyke, J.M. Tour, *J. Phys. Chem. A* 108 (2004) 11151.
- [7] P. Serp, M. Corrias, P. Kalck, *Appl. Catal. A* 253 (2003) 337.
- [8] E. Frackowiak, F. Beguin, *Carbon* 40 (2002) 1775.
- [9] J. Wang, M. Musameh, Y. Lin, *J. Am. Chem. Soc.* 125 (2003) 2408.
- [10] X. Ye, Y. Lin, C.M. Wai, *Chem. Commun.* 5 (2003) 642.
- [11] X. Ye, Y. Lin, C. Wang, C.M. Wai, *Adv. Mater.* 15 (2003) 316.
- [12] B.R. Azamian, K.S. Coleman, J.J. Davis, N. Hanson, M.L.H. Green, *Chem. Commun.* 4 (2002) 366.
- [13] J. Zhang, G. Wang, Y.S. Shon, O. Zhou, R. Superfine, R.W. Murray, *J. Phys. Chem. B* 107 (2003) 3726.
- [14] K. Jiang, A. Eitan, L.S. Schadler, P.M. Ajayan, R.W. Siegel, *Nano Lett.* 3 (2003) 275.
- [15] G.G. Wildgoose, C.E. Banks, R.G. Compton, *Small* 2 (2006) 182.
- [16] X.H. Chen, J.T. Xia, J.C. Peng, W.Z. Li, S.S. Xie, *Compos. Sci. Technol.* 60 (2000) 301.
- [17] B. Yoon, C.M. Wai, *J. Am. Chem. Soc.* 127 (2005) 17174.
- [18] L.M. Ang, T.S.A. Hor, G.Q. Xu, C.H. Tung, S.P. Zhao, J.L.S. Wang, *Carbon* 38 (2000) 363.
- [19] F.Z. Kong, X.B. Zhang, W.Q. Xiong, E. Liu, W.Z. Huang, Y.L. Sun, J.P. Tu, X.W. Chen, *Surf. Coating Technol.* 155 (2002) 33.
- [20] X. Hu, T. Wang, X. Qu, S. Dong, *J. Phys. Chem. B* 110 (2006) 853.
- [21] Z. He, J. Chen, D. Liu, H. Zhou, Y. Kuang, *Diamond Relat. Mater.* 13 (2004) 1764.
- [22] R. Yu, L. Chen, Q. Liu, J. Lin, K.L. Tan, S.C. Ng, *Chem. Mater.* 10 (1998) 718.
- [23] Y. Wang, X. Xu, Z.Q. Tian, Y. Zong, H.M. Cheng, C.J. Lin, *Chem. Eur. J.* 12 (2006) 2542.
- [24] T. Wang, X.G. Hu, X.H. Qu, S.J. Dong, *J. Phys. Chem. B* 110 (2006) 6631.
- [25] Y. Kaneko, N. Iyi, K. Kurashima, T. Matsumoto, T. Fujita, K. Kitamura, *Chem. Mater.* 16 (2004) 3417.
- [26] Q.W. Li, H. Yan, Y. Cheng, J. Zhang, Z.F. Liu, *J. Mater. Chem.* 12 (2002) 1179.
- [27] X.H. Li, J. Zhang, Q.W. Li, H.L. Li, Z.F. Liu, *Carbon* 41 (2003) 598.
- [28] N. Fujiwara, K.A. Friedrich, U. Stimming, *J. Electroanal. Chem.* 472 (1999) 120.
- [29] H. Hitmi, E.M. Belgsir, J.M. Leger, C. Lamy, R.O. Lezna, *Electrochim. Acta* 39 (1994) 407.
- [30] S. Chen, M. Schell, *J. Electroanal. Chem.* 478 (1999) 108.
- [31] J. Shin, W.J. Tornquist, C. Korzeniewski, C.S. Hoaglund, *Surf. Sci.* 364 (1996) 122.
- [32] M.Y. Wang, J.H. Chen, Z. Fan, H. Tang, G.H. Deng, D.L. He, Y.F. Kuang, *Carbon* 42 (2004) 3251.
- [33] H.Q. Song, X.P. Qiu, F.S. Li, W.T. Zhu, L.Q. Chen, *Electrochem. Commun.* 9 (2007) 1416.